Fuelling the obscured star formation at high redshift: surveying the CO(1-0) and HCN(1-0) emission in dusty galaxies

Rybak, M.; Frias Castillo, M.; Hodge, J.A.

Proceedings of the 7th Chile-Cologne-Bonn-Symposium: Physics and Chemistry of Star Formation
V. Ossenkopf-Okada, R. Schaaf, I. Breloy, J. Stutzki (eds.)

FUELLING THE OBSCURED STAR FORMATION AT HIGH REDSHIFT: SURVEYING THE CO(1–0) AND HCN(1–0) EMISSION IN DUSTY GALAXIES

M. Rybak[1, 2], M. Frias Castillo[2] and J. A. Hodge[2]

Abstract. Dusty star-forming galaxies (DSFGs) play a major role in the rapid buildup of the cosmic stellar mass within the first few Gyr after the Big Bang. However, despite concerted efforts, our understanding of the relationship between the diffuse and dense gas reservoirs and star-formation in DSFGs is still limited.

We showcase results of systematic JVLA surveys of the molecular and high-density gas in $z \geq 2$ DSFGs, targeting the CO(1–0) and HCN(1–0) emission, respectively. Our CO(1–0) observations reveal a broad dispersion in gas masses and CO excitation, highlighting the heterogeneity of the most massive, gas-rich DSFG. We find evidence for extended diffuse CO(1–0) halos. The inferred gas fractions and depletion timescales are in a good agreement with the state-of-the-art semi-analytic models. Our HCN(1–0) observations show that unlike present-day ULIRGs, DSFGs have relatively low HCN/CO ratios; despite their massive gas reservoirs, only a small fraction of their molecular gas is in the high-density regime.

1 Introduction

Dusty star-forming galaxies (DSFGs) with star-formation rates (SFRs) of 100's to 1000's $M_\odot$/yr are a major driver of the cosmic star-forming activity at redshift $z \geq 1$ (Casey et al., 2014; Zavala et al., 2021), contributing up to 50% of the total stellar mass and SFR at $z \approx 2$ (Swinbank et al., 2014). These massive, dust-obscured galaxies are bright at sub-mm wavelengths while often invisible in the optical/near-infrared. Despite their importance for our understanding of galaxy evolution, DSFGs have been notoriously difficult to reproduce in cosmological simulations. Consequently, they provide important constraints on our models of galaxy evolution and star formation in the early Universe.

What fuels the vigorous star formation in DSFGs? Are their immense SFRs driven by their massive gas reservoirs, or is their star-forming efficiency enhanced by, e.g., galaxy-galaxy mergers? To understand how the diffuse atomic gas from the intergalactic medium is converted into stars, we need robust measurements of both the total molecular and dense gas content of sizeable samples of DSFGs.

Measuring *total molecular gas masses* of galaxies at high redshift is challenging. The bulk of studies of molecular gas in DSFGs has focused on the bright and easily accessible mid-J CO rotational lines (Tacconi et al., 2020). Yet the inferred gas masses suffer from significant uncertainties. This is because converting the observed mid-J CO line luminosities into gas mass ($M_{\rm mol}$) is a two-step process, as both the CO excitation and the CO(1–0)-to-$M_{\rm mol}$ conversion factor need to be assumed. Moreover, high-resolution studies of individual sources have shown that mid-J CO lines are often much more compact than the CO(1–0) emission. The mid-J CO observations might thus significantly underestimate both the total mass and spatial extent of molecular gas reservoirs in DSFGs.

What do we know about the *dense gas* content of DSFGs? While the number of low-J CO and [CII] detections at high redshift has been rising dramatically over the last decade (e.g., Hodge & da Cunha 2020), these lines trace molecular gas down to densities of few 10^2 cm^{-3}, rather than the dense, star-forming gas ($\geq 10^4$ cm^{-3}). In nearby galaxies, extensive studies have established the HCN emission — particularly the HCN(1–0) line – as a “gold-standard” tracer of dense molecular gas (Gao & Solomon, 2004; Bigiel et al., 2016; Jiménez-Donaire et al., 2019).

However, the number of high-z HCN detections has remained extremely limited. In fact, only two DSFGs have been detected in the HCN(1–0) emission so far (Gao et al., 2007; Oteo et al., 2017), showing

[1] Faculty of Electrical Engineering, Mathematics and Computer Science, Delft University of Technology, The Netherlands , e-mail: m.rybak@tudelft.nl
[2] Leiden Observatory, Leiden University, P.O. Box 9513, 2300 RA Leiden, The Netherlands

©Universität zu Köln 2023, DOI: 10.18716/kups/64624

high HCN(1–0)/CO(1–0) ratios - a proxy for the dense gas fraction. Consequently, it has been hypothesised (Oteo et al., 2017) that the intense star formation in DSFGs is a result of a significant fraction of their molecular gas being in the high-density regime.

In this contribution, we present recent results of on-going systematic surveys of the CO(1–0) and HCN(1–0) emission in high-redshift DSFGs. By measuring both the total molecular gas masses (via CO(1–0)) and dense-gas content (via HCN(1–0)) in a representative samples of DSFGs, these observing programmes present a major milestone in our understanding of the star-forming processes at high redshift.

2 VLA Legacy Library of Molecular Gas at High Redshift

We have conducted a systematic survey of the CO(1–0) emission in a sample of bright $z = 2 - 5$ non-lensed DSFGs using deep JVLA observations. In total, we have targeted 30 galaxies with $S_{850\,\mu\mathrm{m}} \geq$7.5 mJy, selected from wide-field SCUBA-2 imaging (Geach et al., 2017). All targets have spectroscopic redshifts from ALMA or NOEMA spectral scans (Birkin et al., 2021; Chen et al., 2022). By selecting the sources based on the long-wavelength continuum, we are effectively selecting by cold dust mass. As of September 2022, 17 sources have been observed (Frias Castillo, subm.). Out of these, eleven DSFGs have been detected in CO(1–0) with $S/N = 3 - 20$; three additional sources have been tentatively detected ($S/N = 1.5 - 2$).

Despite observing in the most compact, D-array JVLA configuration, we find that the CO(1–0) emission in the majority of our sources extends over $\geq 5''$ (≈40 kpc) scales. We hypothesise that this emission arises from extended, diffuse cold-gas reservoirs that link the central starbursts to the circumgalactic medium. Such extended emission has been hinted at from other studies of cold gas at high redshift: for example, recent ALMA observations have revealed extended, low-surface brightness [CII] halos (e.g., Gullberg et al. 2018; Rybak et al. 2019, 2020; Ginolfi et al. 2020).

To convert the observed CO(1–0) luminosities to gas masses, we adopt $\alpha_{\mathrm{CO}} \equiv M_{\mathrm{H_2}}/L'_{\mathrm{CO(1-0)}} = 1.0$. This value is consistent with constraint from resolved kinematic observations of $z = 2 - 3$ DSFGs (Calistro Rivera et al., 2018; Frias Castillo et al., 2022), although α_{CO} might vary considerably between individual DSFGs (e.g., Harrington et al. 2021). Using this conversion, we find that gas represents 10 – 80% of the total baryonic mass in individual DSFGs, with a median of ≈40%. Despite their large gas masses and potentially extended molecular gas reservoirs, the molecular gas depletion timescales are relatively short, between 80 to 400 Myr (median: 150 Myr).

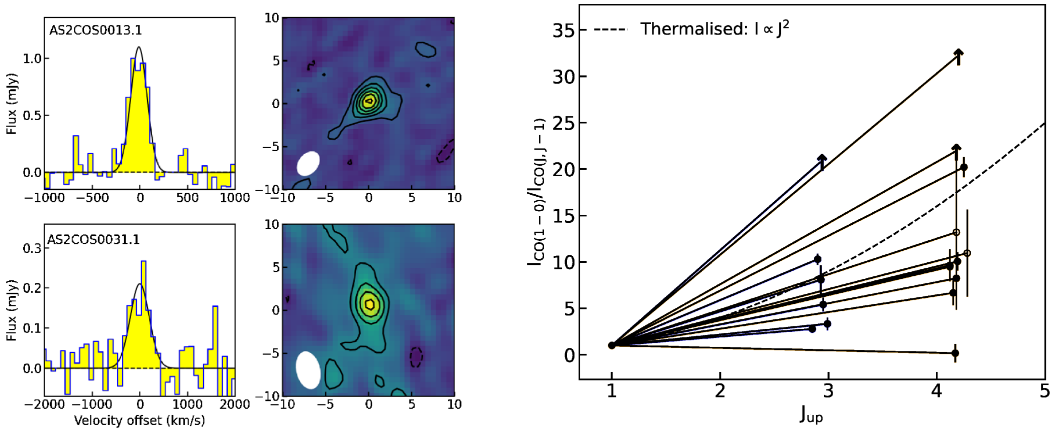

Figure 1: VLA survey of CO(1–0) in unlensed DSFGs - results from the first 17 targets. *Left:* Example CO(1–0) spectra and moment-0 maps, showing clear detections. *Right:* CO(3–2)/CO(1–0) (blue) and CO(4–3)/CO(1–0) (orange) luminosity ratios in our sample, showing the wide range of CO excitation. Several sources are clearly super-thermalised, i.e. fall above the dashed line. Adapted from Frias Castillo et al. (subm.).

Figure 1 shows the CO excitation of our sample. Despite the similarity of galaxies in our sample, the CO(3–2)/CO(1–0) and CO(4–3)/CO(1–0) ratios vary by almost 1 dex. Several sources - including three with

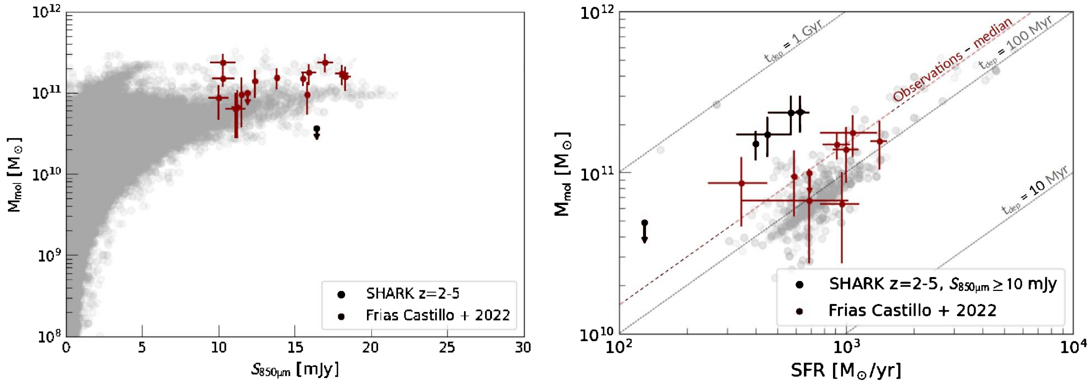

Figure 2: Comparison between our CO(1–0) survey results and simulated $z = 2-5$ DSFGs from the SHARK semi-analytical model. *Left:* 850-μm continuum flux density and molecular gas mass. *Right*: $M_{\rm mol}$ and SFR; our galaxies are consistent with the depletion timescales predicted by SHARK. We find a reasonable agreement between our observation and the simulation without a need to tune either the $\alpha_{\rm CO}$ conversion factor or the semi-analytical model. Adapted from Frias Castillo et al. (subm.).

CO(1–0) non-detections - have a super-thermalised CO ladder. We do not see any significant correlation between CO excitation and SFR, total gas mass, or the offset from the main sequence; the only tentative trend is with SFR surface density ($\Sigma_{\rm SFR}$). The large scatter in CO excitation highlights the pitfalls of estimating the molecular gas mass from mid-J CO emission lines.

Finally, we compare our observational results to the $z = 2-5$ DSFGs from the SHARK semi-analytic models (Lagos et al., 2018, 2020). The SHARK models have been able to reproduce many key aspects of the high-z DSFG population, including number counts and redshift distribution. For a comparison with our sample, we select SHARK galaxies at $z = 2$ to 5, with the 850-μm flux density higher than 10 mJy. As shown in Fig. 2, we find a surprisingly good agreement between the properties of our targets and SHARK DSFGs; the two samples are broadly consistent in terms of SFR, $M_\star$, and $M_{\rm mol}$. In particular, we find that the bulk of our sample has molecular gas depletion timescales of $t_{\rm dep} \approx 100$ Myr, similar to the SHARK sample. Curiously, this agreement is facilitated by our choice of $\alpha_{\rm CO} = 1.0$; adopting a Milky-Way-like $\alpha_{\rm CO} = 4.4$ would lead to a significant discrepancy between the "real" and SHARK DSFGs.

3 PRUSSIC - a comprehensive survey of dense gas tracers in DSFGs

To provide a comprehensive overview of dense gas content in high-redshift DSFGs, we have launched PRUSSIC - a concerted JVLA, ALMA, and NOEMA survey. Our JVLA observations targeted the HCN(1–0) emission at high redshift, targeting six $z \sim 3$ gravitationally lensed DSFGs (Rybak et al., 2022) - the largest and deepest survey of HCN(1–0) at high redshift to date. The depth of the observations would allow $S/N \geq 3$ HCN(1–0) detections down to HCN/CO ratios - i.e, dense-gas fractions - of a few per cent. Such deep observations can be only obtained for strongly lensed galaxies, as the HCN(1–0) line is often 1–2 dex fainter than low-J CO emission. Surprisingly, out of the six targets, only a single DSFG was detected in HCN(1–0) (at $\sim 4.4\sigma$), with another tentatively detected in the HCO^+(1–0) emission. Even after stacking the data in the spectral domain, we do not detect any significant HCN(1–0) emission - implying a mean HCN(1–0)/CO(1–0) ratio of ≤ 0.045.

The surprisingly low HCN/CO ratios contrast with previous claims of high HCN/CO ratios in DSFGs. To understand this dichotomy, we re-examined the two previous detections from Gao et al. (2007) and Oteo et al. (2017) with high claimed HCN/CO ratios: J16359 (HCN/CO$\sim$0.15) and SDP.9 (HCN/CO$\sim$0.3). For J16359, the updated CO(1–0) measurements bring the HCN/CO ratio down to $\sim$0.1, bringing it more in line with our results. SDP.9 has a very compact continuum morphology (<300 pc diameter) and an X-ray luminous AGN (Massardi et al., 2018). Consequently, the HCN luminosity in SDP.9 might be boosted by the central AGN.

In addition, we see tentative evidence for DSFGs having lower HCN/FIR ratios than expected from $z \sim 0$

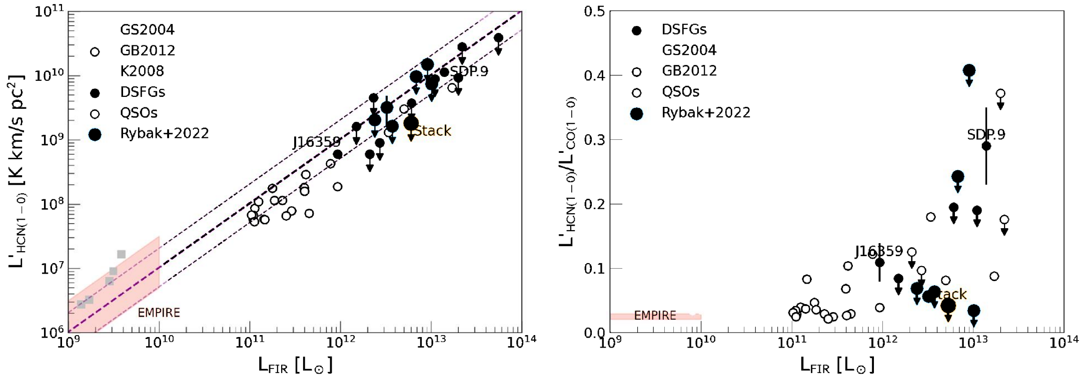

Figure 3: *Left:* HCN-FIR luminosity correlation on $z \sim 0$ and high-redshift galaxies. The individual DSGGs from Rybak et al. (2022) are highlighted in blue; the upper limit from the stacked spectrum is shown in orange. *Left*: Dense-gas fractions (i.e., HCN/CO) in high-z DSFGs, compared to $z \sim 0$ studies. The Rybak et al. (2022) observations imply that DSFGs have dense-gas fractions similar to $z \sim 0$ spiral galaxies, rather than ULIRGs. Adapted from Rybak et al. (2022).

empirical trends. Namely, while the single detection is consistent with the trend from Jiménez-Donaire et al. (2019), some of the upper limits and the stack spectrum fall below the $\pm 1\sigma$ region (Fig. 3). This indicates that DSFGs have elevated dense-gas star-forming efficiency. In other words, while they might have relatively lower amounts of dense gas, they convert it to stars more efficiently than, e.g., nearby ULIRGs[1].

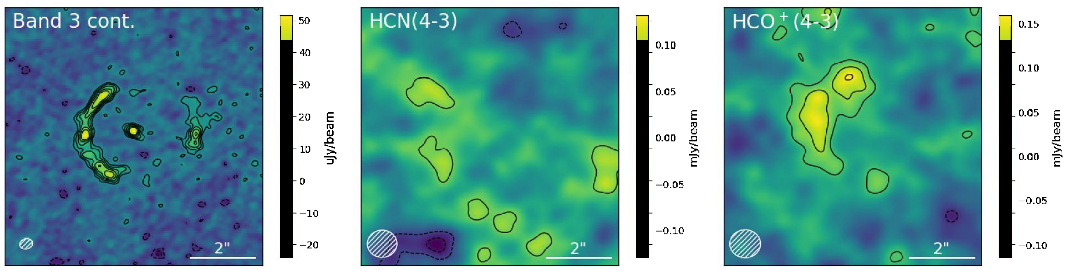

Figure 4: ALMA imaging of SDP.81. *Left to right*: Band 3 (3-mm) continuum, HCN(4–3), and HCO^+(4–3) emission. The contours in HCN/HCO^+ images start at 2σ and increase by 1σ. While the HCN(4–3) line is below the detection threshold, HCO^+(4–3) is both detected and spatially resolved. SDP.81 has an unusually high HCO^+/HCN ratio of ≥ 6.5, potentially due to a sub-solar metallicity.

We are supplementing these JVLA observations by ALMA and NOEMA programmes targeting the mid-J HCN, HCO^+, and HNC lines. The mid-J lines are often intrinsically brighter than the $J_{\rm up} = 1$ transitions and fall into the easily-accessible 3-mm atmospheric window, making them potentially appealing tracers of dense-gas content and chemistry in DSFG. While mid-J HCN/HCO^+/HNC lines have been detected in a handful of DSFGs (Danielson et al., 2011; Béthermin et al., 2018; Cañameras et al., 2021), we are dramatically expanding the number of detections, with eight DSFGs detected in the HCN(3–2) and (4–3) transitions so far (Rybak et al., in prep.). As an example, Fig. 4 shows high-resolution ALMA Band 3 imaging of SDP.81, a well-studied, strongly lensed $z \sim 3$ DSFG. While the HCN(4–3) line is not detected, HCO^+(4–3) is both detected and resolved. We find that SDP.81 has an unusually high HCO^+/HCN ratio of ≥ 6.5 (3σ limit), comparable to nearby low-metallicity environments such as 30 Doradus.

[1] Here, we assume the "standard" conversion factor between the HCN luminosity and dense gas mass: $M_{\rm dense} = 10 M_\odot / L_\odot \times L_{\rm HCN}$. This conversion factor remains poorly constrained, both at low and high redshift.

Acknowledgements

M. R. is supported by the NWO Veni project "Under the lens" (VI.Veni.202.225). M. F. C. and J. H. acknowledge support of the VIDI research programme with project number 639.042.611, which is (partly) financed by the Netherlands Organisation for Scientific Research (NWO).

References

Béthermin, M., Greve, T. R., De Breuck, C., et al. 2018, A&A, 620, A115, doi:10.1051/0004-6361/201833081
Bigiel, F., Leroy, A. K., Jiménez-Donaire, M. J., et al. 2016, ApJ, 822, L26, doi:10.3847/2041-8205/822/2/L26
Birkin, J. E., Weiss, A., Wardlow, J. L., et al. 2021, MNRAS, 501, 3926, doi:10.1093/mnras/staa3862
Cañameras, R., Nesvadba, N. P. H., Kneissl, R., et al. 2021, A&A, 645, A45, doi:10.1051/0004-6361/202038979
Calistro Rivera, G., Hodge, J. A., Smail, I., et al. 2018, ApJ, 863, 56, doi:10.3847/1538-4357/aacffa
Casey, C. M., Narayanan, D., & Cooray, A. 2014, Physics Reports, 541, 45, doi:10.1016/j.physrep.2014.02.009
Chen, C.-C., Liao, C.-L., Smail, I., et al. 2022, ApJ, 929, 159, doi:10.3847/1538-4357/ac61df
Danielson, A. L. R., Swinbank, A. M., Smail, I., et al. 2011, MNRAS, 410, 1687, doi:10.1111/j.1365-2966.2010.17549.x
Frias Castillo, M., Rybak, M., Hodge, J., et al. 2022, ApJ, 930, 35, doi:10.3847/1538-4357/ac6105
Gao, Y., Carilli, C. L., Solomon, P. M., & Vand en Bout, P. A. 2007, ApJ, 660, L93, doi:10.1086/518244
Gao, Y. & Solomon, P. M. 2004, ApJSS, 152, 63, doi:10.1086/383003
Geach, J. E., Dunlop, J. S., Halpern, M., et al. 2017, MNRAS, 465, 1789, doi:10.1093/mnras/stw2721
Ginolfi, M., Jones, G. C., Béthermin, M., et al. 2020, A&A, 633, A90, doi:10.1051/0004-6361/201936872
Gullberg, B., Swinbank, A. M., Smail, I., et al. 2018, ApJ, 859, 12
Harrington, K. C., Weiss, A., Yun, M. S., et al. 2021, ApJ, 908, 95, doi:10.3847/1538-4357/abcc01
Hodge, J. A. & da Cunha, E. 2020, Royal Society Open Science, 7, 200556, doi:10.1098/rsos.200556
Jiménez-Donaire, M. J., Bigiel, F., Leroy, A. K., et al. 2019, ApJ, 880, 127, doi:10.3847/1538-4357/ab2b95
Lagos, C. d. P., da Cunha, E., Robotham, A. S. G., et al. 2020, MNRAS, 499, 1948, doi:10.1093/mnras/staa2861
Lagos, C. d. P., Tobar, R. J., Robotham, A. S. G., et al. 2018, MNRAS, 481, 3573, doi:10.1093/mnras/sty2440
Massardi, M., Enia, A. F. M., Negrello, M., et al. 2018, A&A, 610, A53, doi:10.1051/0004-6361/201731751
Oteo, I., Zhang, Z. Y., Yang, C., et al. 2017, ApJ, 850, 170, doi:10.3847/1538-4357/aa8ee3
Rybak, M., Calistro Rivera, G., Hodge, J. A., et al. 2019, ApJ, 876, 112, doi:10.3847/1538-4357/ab0e0f
Rybak, M., Hodge, J. A., Greve, T. R., et al. 2022, A&A, 667, A70, doi:10.1051/0004-6361/202243894
Rybak, M., Hodge, J. A., Vegetti, S., et al. 2020, MNRAS, 494, 5542, doi:10.1093/mnras/staa879
Swinbank, A. M., Simpson, J. M., Smail, I., et al. 2014, MNRAS, 438, 1267, doi:10.1093/mnras/stt2273
Tacconi, L. J., Genzel, R., & Sternberg, A. 2020, ARA&A, 58, 157, doi:10.1146/annurev-astro-082812-141034
Zavala, J. A., Casey, C. M., Manning, S. M., et al. 2021, ApJ, 909, 165, doi:10.3847/1538-4357/abdb27